Sustainable Solutions in Structural Engineering and Construction
Edited by Chantawarangul, K., Suanpaga, W., Yazdani, S., Vimonsatit, V., and Singh, A.

ISBN: 978-0-9960437-0-0

WIND LOADS AND WIND-INDUCED BUCKLING OF OPEN-TOPPED OIL-STORAGE TANKS IN VARIOUS ARRANGEMENTS

YASUSHI UEMATSU [1], JUMPEI YASUNAGA[2], and CHOONGMO KOO [3]

[1] *Dept of Architecture and Building Science, Tohoku University, Sendai, Japan*
[2]*Steel Research Laboratory, JFE Steel Corporation, Kawasaki, Japan*
[3]*MIDAS IT Japan, Tokyo, Japan*

Wind force coefficients for designing open-topped oil-storage tanks in various arrangements have been investigated under experiments involving a wind tunnel and a buckling analysis of the tanks. In the wind tunnel experiment, the wind pressures were measured simultaneously at many points both on the external and internal surfaces of a rigid model for various arrangements of two to four tanks. The effects of arrangement and gap spacing of tanks on the pressure distribution are investigated. The buckling of tanks under static wind loading is analyzed by using a non-linear finite element method. A discussion of the effect of wind force distribution on the buckling behavior follows. The authors provided a model of circumferential distribution of wind force coefficient on isolated open-topped tanks in their previous paper. This paper proposes a model of wind-force coefficient for plural tanks in various configurations by modifying the model for isolated tanks.

Keywords: Wind pressure, Wind tunnel experiment, Internal pressure, Finite element analysis.

1 INTRODUCTION

Open-topped oil-storage tanks are composed of thin curved panels. Buckling may occur when they are subjected to wind loads in the empty or partially-filled state. Therefore, wind-induced buckling is one of the most important technological problems when designing these tanks. Yasunaga *et al.* (2012a, 2012b) discussed the wind loads for isolated tanks based on pressure measurements in a wind tunnel, as well as on a finite-element analysis of the buckling of tanks, and found that the distribution of positive wind force (or pressure difference) coefficient in the windward area affected the buckling behavior significantly. They proposed a model of the design wind pressure coefficients on tanks, focusing on the buckling behavior.

In practical situations, however, more than two tanks are constructed in various configurations. In the present study, a wind tunnel experiment was carried out with two to four models, in order to investigate the effects of the configuration and gap spacing between tanks on the external and internal pressures, and the resultant buckling behavior of the tanks. Based on the results, we propose a model of wind force coefficient for plural tanks in various configurations by modifying the model for isolated tanks. It should be noted that the present paper is an extended version of our

previous paper (Uematsu *et al.* 2013), in which the focus was only on the wind pressure distributions.

2 WIND TUNNEL EXPERIMENT

2.1 Experimental apparatus and procedure

The wind tunnel experiment was carried out in a closed-circuit-type wind tunnel with a working section 18.1 m long, 2.5 m wide, and 2.0 m high. A turbulent boundary layer with a power law exponent of 0.15 for the mean wind velocity profile was generated on the wind tunnel floor. Three models, named Models A to C, with different aspect ratios of H/D = 1.0, 0.5, and 0.25 were used; the external diameter D and wall thickness of the models are 250 mm and 6 mm, respectively. The geometric scale of the models is assumed to be 1/400, same as that of the wind-tunnel flow. The wind velocity U_H at the level of model height H was approximately 10 m/s; the corresponding Reynolds number Re defined in terms of U_H and D is approximately 1.7×10^5.

Figure 1 shows the arrangements of models tested, in which the shaded circles represent dummy models with no pressure taps, and are the same shape as those of the instrumented model (white circle). The arrangement of models is represented by wind direction (β or β^*) and gap spacing (S) between models. The non-dimensional gap spacing S/D ranged from 0.125 to 1.0. The pressure taps of 0.5 mm diameter were installed at a step of 15° on the external surface, and at a step of 30° on the internal surface along the circumferences at several heights. The pressure taps were connected to pressure transducers in parallel via 80 cm lengths of flexible vinyl tubing of 1 mm inside diameter. The wind pressures at all taps were sampled simultaneously at a rate of 1 kHz for approximately 33 sec. The compensation for the frequency response of the pneumatic tubing system was carried out by using a digital filter, to obtain a flat response up to approximately 500 Hz. From the experimental data, four or five series of full-scale 10-min time history of pressures were obtained. The statistical values of wind pressures were evaluated by applying an ensemble average to the results of these consecutive runs. The wind pressure was normalized by the dynamic pressure q_H of the flow at a height of H, and expressed as the wind pressure coefficient.

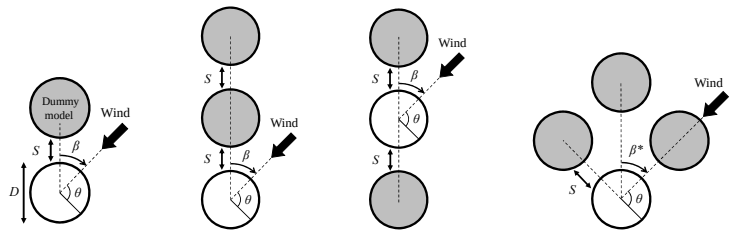

I (β = 0 – 180°) II (β = 0 – 180°) III (β = 0 – 90°) IV (β^* = 0 – 180°)

Figure 1. Configuration of models.

2.2 Results of the External Pressure Coefficients

Since the variation of mean and standard deviation pressure coefficients, C_{pe_mean} and C_{pe_rms}, in the vertical direction is small, the focus in this paper is on the circumferential distribution at a reference height z_{ref} that provided the maximum external pressure in the isolated model case; i.e., z_{ref}/H = 0.80, 0.67 and 0.61 for Models A, B and C, respectively.

2.2.1 *Two or three models in an in-line arrangement*

The pressure distribution changes with wind direction (β or β^*) and S/D, significantly. Regarding the wind pressure distributions, the main findings from the wind tunnel experiment may be summarized as follows: (1) With a decrease in the aspect ratio H/D, the magnitude of C_{pe_mean}, both positive and negative, becomes smaller. (2) When $S/D \geq 1.0$, the pressure distribution is similar to that for an isolated model, except for $\beta \leq 30^o$. When $\beta \leq 30^o$, the C_{pe_mean} values are small in magnitude, while the C_{pe_rms} values are large. This feature is due to a shielding effect and vortex shedding from the upstream model. (3) Even when β = 0° (tandem arrangement), the circumferential C_{pe_mean} distribution on the downstream model becomes asymmetric with respect to θ = 0° for Models B and C. This feature implies that the flow around models in the tandem arrangement is quite sensitive to a small perturbation, when the aspect ratio H/D is relatively small.

Furthermore, it was found that the magnitude and extent of positive wind pressures in the windward area were affected by wind direction and gap spacing. Yasunaga *et al.* (2012b) indicated that the distribution of positive wind pressure coefficients affected the buckling behavior of tanks significantly. Therefore, the characteristics of positive pressures in the windward area are investigated in more detail. Figure 2 shows the range θ_0 of positive C_{pe_mean} values plotted against S/D. The value of θ_0 is almost the same as that for the isolated model (dashed line) when $S/D \geq 1.0$. With a decrease in S/D, the value of θ_0 increases or decreases, depending on β. The value of θ_0 is very large when β = 90°, which may result in a reduction of buckling load of tanks.

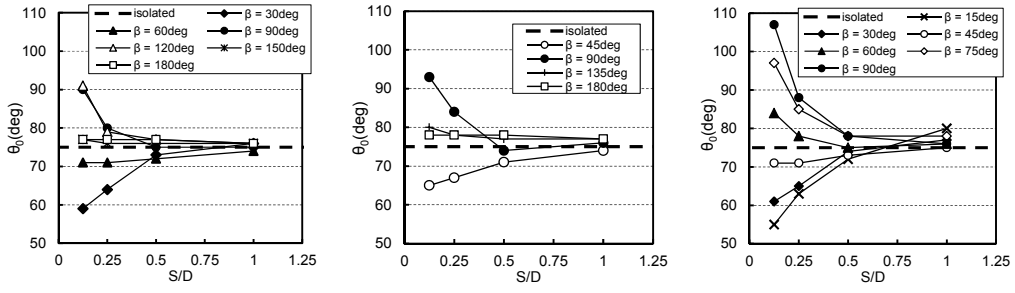

(a) Arrangement I (b) Arrangement II (c) Arrangement III

Figure 2. Range of positive C_{pe_mean} values in the windward area plotted against S/D.

2.2.2 *Four models in rectangular arrangement*

Figure 3 shows typical results on the C_{pe_mean} distribution for Arrangement IV, in which the results are compared with those for two models (Arrangement I). It is found that both results are similar to each other, particularly for the positive C_{pe_mean} distribution. This feature implies that the C_{pe_mean} distribution for many tanks in a rectangular arrangement can be evaluated from that for two models (Arrangement I).

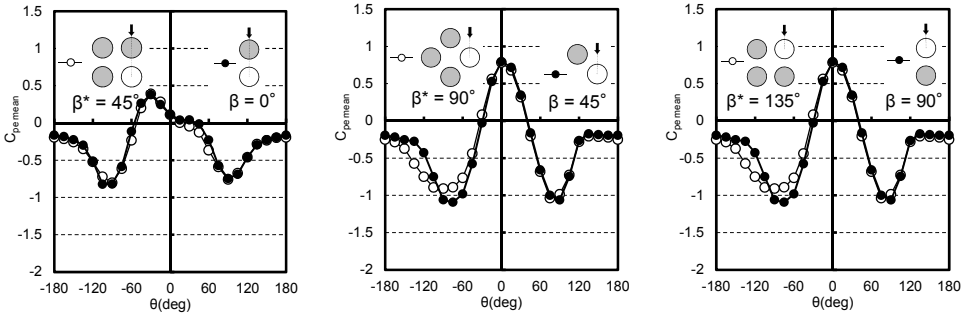

(a) Case 1 (b) Case 2 (c) Case 3

Figure 3. Distributions of C_{pe_mean} for Arrangements I and IV.

2.3 Results on the Internal Pressure Coefficients

Since the variation of the C_{pi_mean} value is small both in the vertical and circumferential directions, the focus in this paper is on the averaged value (C_{pi_area}) over the whole internal surface. Figure 4 shows the variation of C_{pi_area} with S/D. With a decrease in S/D, the difference from that for the isolated model becomes more significant. In the case of in-line arrangement, the value of C_{pi_area} becomes the minimum when $\beta = 90°$. Considering that the positive C_{pe_mean} values in the windward area are large, and the negative C_{pi_area} values are also large in magnitude when $\beta = 90°$, it may be concluded that a wind direction perpendicular to the line of arrangement provides a critical condition of wind force distribution from the viewpoint of buckling. On the other hand, in the case of a rectangular arrangement, the value of C_{pi_area} was smaller in magnitude than that for the isolated tank. Therefore, the effect of internal pressure on the buckling load seems to be relatively small compared with the in-line arrangement.

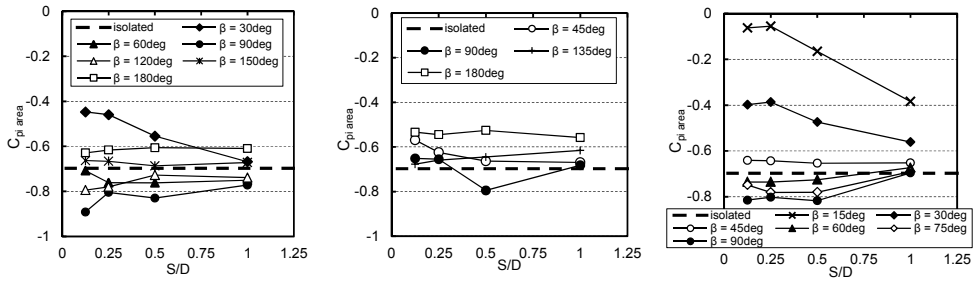

(a) Arrangement I (b) Arrangement II (c) Arrangement III

Figure 4. Area-averaged mean internal pressure coefficient plotted against S/D.

3 FINITE ELEMENT ANALYSIS OF BUCKLING BEHAVIOR

3.1 Method of Analysis

Based on a wind tunnel experiment with an isolated tank model, Yasunaga *et al*. (2012a) showed that the mean wind force coefficient can be used for evaluating the design wind loads on open-topped tanks. Therefore, the focus in this paper is on the deflection and buckling behavior of tanks under static wind loading.

A nonlinear finite element analysis of the buckling of tanks is made by using a computer program "MSC.Marc". The analytical model is the same as one of the experimental models that Yasunaga *et al*. (2012b) used in their previous study. The model is made of polyester film with Young's modulus E = 5.55 GPa and Poisson's ratio ν = 0.3. The diameter D, height H, and thickness t are 216 mm, 90 mm, and 0.1 mm, respectively. Both ends are assumed to be clamped to rigid rings.

The arc-length method is used in the analysis. The representative wind load p is given by the wind force per unit area at the stagnation point (= $q_H \cdot C_{fs}$, with C_{fs} being the wind force coefficient at the stagnation point). The buckling load p_{cr} is defined by a load providing the maximum point of the equivalent path. It is normalized as follows:

$$\lambda_{cr} = \frac{p_{cr} R^3}{D_b}, \; D_b = \frac{Et^3}{12(1-\nu^2)} \qquad (1), (2)$$

where R and D_b represent the radius and flexural rigidity of the tank, respectively.

Analysis is made for three kinds of wind force distributions. The first is the actual distribution obtained from the wind tunnel experiment (Load Case 1); the second is the averaged distribution over the whole height (Load Case 2); and the third is an imaginary distribution that is provided by replacing the negative wind force coefficients in Load Case 2 by zero (Load Case 3).

3.2 Results of Analysis

Table 1 shows the results for the non-dimensional buckling loads λ_{cr} for β = 90° in Arrangement I. The results for the isolated model are also shown for the purpose of comparison. In the table, θ_0^* represents the range of positive wind force coefficient. The value of λ_{cr} for Load Case 2 is generally smaller than that for Load Case 1. This is due to the effect of vertical distribution of wind force coefficient C_f in the windward area. On the other hand, the value of λ_{cr} for Load Case 3 is similar to that for Load Case 2, despite a significant difference in the C_f distribution in the side and leeward areas. This feature implies that the buckling behavior is mainly affected by the magnitude and extent of the positive C_f values in the windward area. In other words, the negative C_f values in the side and leeward areas minutely affect the buckling behavior. It is found that the buckling load decreases with an increase in θ_0^*. The buckling deflection, not shown here to save space, concentrates in the positive C_f area.

Table 1. Non-dimensional buckling loads λ_{cr} (Arrangement I, $\beta = 90^{o}$).

S/*D*	Load Case			θ_0^*
	1	2	3	(deg)
1.0	705	658	657	122
0.5	698	654	653	124
0.25	690	649	650	129
0.125	678	642	641	132
Isolated model	704	654	–	122

4 DESIGN WIND PRESSURE COEFFICIENTS

Yasunaga et al. (2012b) proposed models of external and internal pressure coefficients, C_{pe} and C_{pi}, as a function of H/D for isolated tanks. In the present paper, the same model of C_{pe} is used, while the model of C_{pi} is modified so that the extent of positive wind force coefficient C_f (= C_{pe} – C_{pi}) coincides with the experimental result. The models of C_{pi} for three locations A to C are provided as shown in Figure 5.

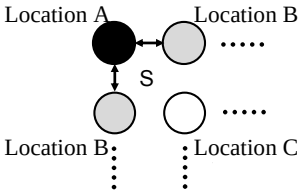

Location A: $C_{pi} = -0.67 - 0.50(H/D) + 0.32(S/D)$

Location B: $C_{pi} = -0.69 - 0.50(H/D) + 0.34(S/D)$

Location C: $C_{pi} = -0.35 - 0.50(H/D)$

Figure 5. Model of internal pressure coefficient.

5 CONCLUDING REMARKS

The wind pressure distribution on open-topped oil-storage tanks in various arrangements were measured in a turbulent-boundary layer. Based on the result, a model of internal pressure coefficient is provided as a function of H/D and S/D for three representative locations of tanks, which can be combined with the model of external pressure coefficient that Yasunaga et al. (2012b) proposed for isolated tanks.

References

Uematsu, Y., and Yasunaga, J., Wind Loads on Open-topped Oil-storage Tanks in Various Arrangements, *Proc. 6th European and African Conference on Wind Engineering*, Cambridge, UK, 7-11 July 2013.

Yasunaga, J., Koo, C. and Uematsu, Y., Wind loads for designing cylindrical storage tanks Part 1 Characteristics of wind pressure and force distributions, *J. Wind Eng.*, JAWE, 37(2), 43-53, 2012a (in Japanese).

Yasunaga, J., Koo, C. and Uematsu, Y., Wind loads for designing cylindrical storage tanks Part 2 Wind force model with consideration of the buckling behavior under wind loading, *J. Wind Eng.*, JAWE, 37(3), 79-92, 2012b (in Japanese).